Inorganic Chemistry

pubs.acs.org/IC

Article

Antitumor Effect of Organometallic Half-Sandwich Ru(II)−Arene Complexes Bearing a Glutathione *S*-Transferase Inhibitor

Tianyu Han, Yuying Wu, Weinan Han, Kaiwen Yan, Jian Zhao, and Yanyan Sun*

Cite This: https://doi.org/10.1021/acs.inorgchem.1c01482

Read Online

ACCESS | Metrics & More | Article Recommendations | Supporting Information

ABSTRACT: The facile modification of the ligands in organometallic Ru(II)−arene complexes offers more opportunities to optimize their pharmacological profiles. Herein, three Ru(II)−arene complexes containing a glutathione *S*-transferase (GST) inhibitor (NBDHEX) in chelate ligand have been designed and synthesized in this study. In vitro results indicated that the ligation with NBDHEX significantly increased the activities and selectivities of the organometallic Ru(II)−arene complexes against tumor cells, especially complex **3**, which was the most active compound among the tested compounds. DFT calculations and hydrolysis results demonstrated that complex **3** with more alkyl groups in the arene ligand has increased electron density at the Ru(II) center as compared with complexes **1** and **2**, thus resulting in the improved hydrolysis rate, which may be responsible for its higher anticancer activity. Further studies showed that complexes **1**−**3** can cause the loss of the mitochondrial membrane potential and upregulate the expression of Bcl-2 and Bax in A549 cells, suggesting that complexes **1**−**3**-induced cell death may be mediated via the mitochondrial apoptotic pathway. Thus, these findings suggested that simultaneous modification of the chelate ligands and arene rings in the organometallic Ru(II)−arene complexes is an effective way to improve their pharmacological properties.

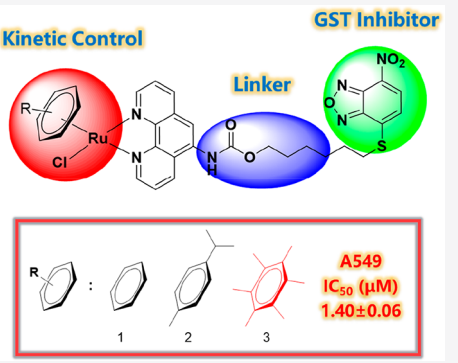

INTRODUCTION

Platinum(II)-based anticancer drugs represent one of the important chemotherapy agents that have been widely used for the treatment of solid tumors.[1] These platinum complexes show unique advantage in the field of tumor therapy due to their covalently binding to the target DNA, a character that is different from most of the organic drugs, thus prolonging the drug action duration and improving the therapeutic efficacy by completely inhibiting the bioactivity of the therapeutic target.[2] However, the irreversible binding of the platinum drugs to DNA may result in severe side effects. In addition, the inevitable drug resistance is another limitation of the platinum drugs.[3] Considering the disadvantages of platinum drugs, other metal-based anticancer compounds have been designed as alternatives to platinum drugs, especially ruthenium-based anticancer agents, which has shown great promising in cancer therapy due to their unique biological properties and low toxicity.[4−19]

To date, three ruthenium complexes, including two chemotherapy agents (NAMI-A, KP1019, and its sodium salt KP1339) and one photosensitizer (TLD1433), have been approved for clinical trials, especially KP1339 and TLD1433, both of which have successfully completed phase I clinical trials with encouraging profiles (Figure 1).[20−23] However, the clinical studies of NAMI-A were interrupted due to the unconvincing efficacy.[24,25] Recently, the organometallic half-sandwich ruthenium(II) complexes have attracted increasing attention for their potential clinical applications in cancer therapy. The notable examples are RM175 and RAPTA-C, which were developed by the groups of Sadler and Dyson, respectively, and are currently in an advanced preclinical stage.[26−29] Importantly, the facile modification of the coordination ligands and arene rings in Ru(II)−arene compounds offers more opportunities to optimize their pharmacological profiles with improved anticancer activity and selectivity.[30−35]

Glutathione *S*-transferase(s) (GSTs) are a class of phase II detoxification enzymes that catalyze the conjugation of glutathione (GSH) with both endogenous and exogenous electrophilic substrates, thus leading to the inactivation of various electrophilic agents, including anticancer drugs.[36] Moreover, overexpression of GSTs was detected in many types of human tumors, which would accelerate the degradation of anticancer drugs before they reach the therapeutic targets.[37] Consequently, GST inhibitors based on different chemical structures, such as benzoxadiazole, dichlorotriazine, and α-chloroacetamide, have been developed as potential anticancer agents.[38,39] Besides, several natural

Received: May 16, 2021

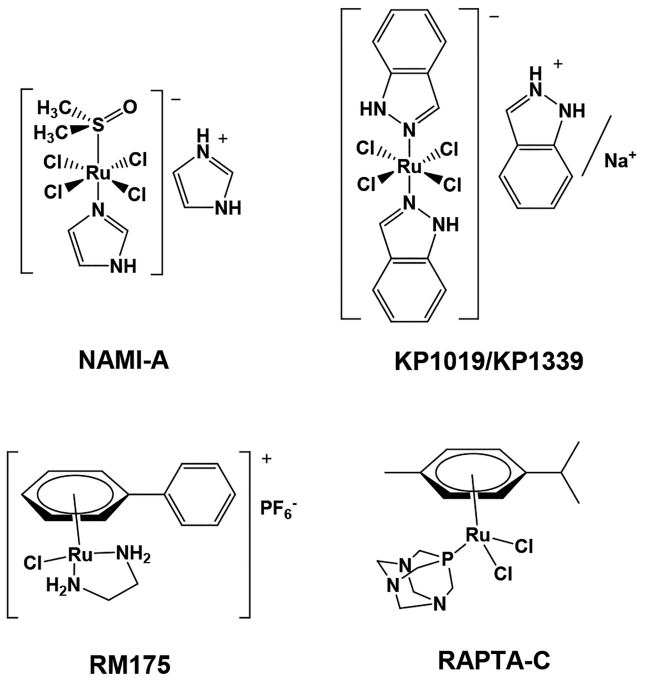

Figure 1. Related anticancer ruthenium complexes in this paper.

compounds such as piperlongumine and curcumin have also shown the potent cytotoxicity by inhibiting the activity of GSTs.[40,41] Noteworthy, many studies have demonstrated that GST inhibitors can not only potentiate the cytotoxicity of the chemotherapeutic agents against the cancer cells but also resensitize the efficacy of the chemotherapeutic agents against drug-resistant cancer cells, implying the positive synergistic effect between GST inhibitors and chemotherapeutic agents in the aspect of cancer therapy.[42−46] More importantly, the complexation with ethacrynic acid (a potent GSTs inhibitor) conferred the metal-based chemotherapeutic agents including platinum(IV), ruthenium(II), and osmium(II) complexes with higher potential to potentiate their cytotoxicity and overcome the drug resistance,[47,48] highlighting that hybridization of GST inhibitors with metal-based cytotoxic agents is a rational and effective way for the design of novel anticancer agents.

Nitrobenzoxadiazole (NBD) derivatives are a class of effective GST inhibitors, and the notable example is 6-(7-nitro-2,1,3-benzoxadiazol-4-ylthio)hexanol (NBDHEX), which has been widely studied and modified as a GST inhibitor.[49−51] For example, it has been described that the modifications on the hydroxy-containing alkyl chain with different linker lengths and number of oxygen atoms at the C4 position of the NBD scaffold can modulate the physicochemical properties (e.g., hydrophilicity/hydrophobicity balance) as well as cytotoxicity of NBDHEX.[52,53] Moreover, it has been shown that NBDHEX has the synergistic effect with platinum-based agents against cancer cells.[44] Herein, three arene−Ru(II) GST inhibitor conjugates have been designed and synthesized by introduction of NBDHEX in the organometallic Ru(II) scaffold (Scheme 1). It is anticipated that NBDHEX can potentiate the cytotoxicity of the organometallic Ru(II)−arene complexes, while the arene ligands can modulate their physicochemical properties such as kinetic reactivity. Therefore, the hydrolysis rates, biological activities, and underlying anticancer mechanisms of the prepared arene−Ru(II) conjugates will be studied and discussed.

RESULTS AND DISCUSSION

Synthesis and Characterization. Ligand **L1** and complexes **1**−**3** were synthesized by following the procedure shown in Scheme 1. First, 5-aminophenanthroline was mixed with *N*,*N*-diisopropylethylamine (DIPEA) and a catalytic amount of 4-(dimethylamino)pyridine (DMAP) and then reacted with triphosgene following by adding NBDHEX to yield ligand **L1**. Complexes **1**−**3** were subsequently prepared by the reaction of the dimer $[Ru(arene)Cl_2]_2$ with **L1** (arene = benzene, *p*-cymene, and hexamethylbenzene). The resulting complexes were characterized by elemental analysis as well as ^1H and ^{13}C NMR spectra along with ESI-MS spectrometry (see the Supporting Information, Figures S1−S12). The spectral data were in good agreement with the corresponding structures of complexes **1**−**3**. The fluorescence emission spectra (Ex = 430 nm) were also analyzed (see Figure S13),

Scheme 1. Preparation of Ligand L1 and Complexes 1−3[a]

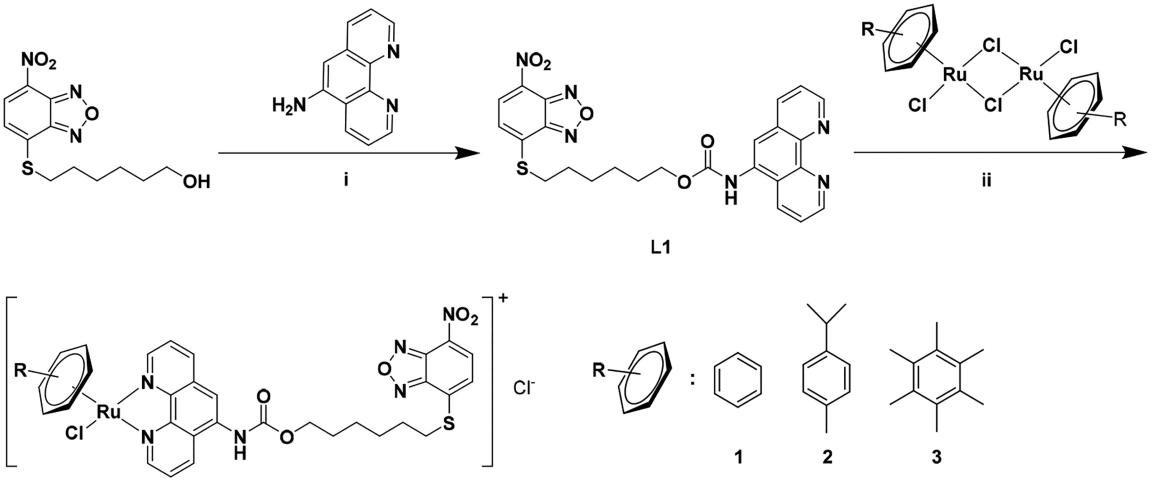

[a]Reagents and conditions: (i) DIPEA, DMAP, DCM, 0 °C; N_2, triphosgene, 0 °C, 4 h; EtOH, rt, 4 h; (ii) EtOH, rt, 5 h.

https://doi.org/10.1021/acs.inorgchem.1c01482
Inorg. Chem. XXXX, XXX, XXX−XXX

Table 1. log P_{OW} and IC_{50} Values of the Ligand L1, Complexes 1−3, Ru-Con, and Cisplatin against A549, MCF-7, and LO2 Cell Lines after 72 h Incubation

		IC_{50} values (μM)				
compound	log P_{OW}	A549	SF[a]	MCF-7	SF	LO2
1	−0.64	2.80 ± 0.14	7.3	9.99 ± 0.44	2.1	20.49 ± 1.42
2	−0.37	2.42 ± 0.11	6.7	8.38 ± 0.31	1.9	16.17 ± 0.98
3	−0.28	1.40 ± 0.06	17.6	5.23 ± 0.16	4.7	24.69 ± 1.74
L1	6.05	3.14 ± 0.14	0.8	11.09 ± 0.58	0.2	2.58 ± 0.09
Ru-Con	n.d.[b]	22.71 ± 1.12	1.9	13.50 ± 0.75	3.1	42.27 ± 1.94
cisplatin	−2.03[c]	19.43 ± 0.84	0.5	10.98 ± 0.64	0.9	10.11 ± 0.62

[a]SF (sensitivity factor) = IC_{50} (normal cell line)/IC_{50} (tumor cell line); the average of three experiments was taken for all results. [b]n.d. = not determined. [c]Cited from ref 18.

showing that the emission wavelength of complexes **1**−**3** was 530 nm.

Moreover, the log P_{OW} values of **L1** and complexes **1**−**3** were determined by using shake-flask method followed by UV−vis analysis. As shown in Table 1, the log P_{OW} values of ruthenium complexes **1**−**3** were in the appropriate range of −0.64 to −0.28, which were much lower than that of ligand **L1** (6.05), indicating that complexes **1**−**3** possessed moderate lipophilicity, and hydrophilicity was beneficial for the druggability of the resulting complexes.

In Vitro Cytotoxic Activity. The cytotoxic activities of ligand **L1** and complexes **1**−**3** against MCF-7 (breast cancer), A549 (nonsmall cell lung cancer), and normal liver cell line LO2 were evaluated by an MTT assay together with [(η^6-*p*-cymene)Ru(1,10-phenanthroline-κN^1,κN^{10})Cl]Cl (abbreviated as Ru-con) and cisplatin as positive control after 72 h incubation. After three parallel experiments, the IC_{50} values (the dose required to inhibit 50% cell growth) were determined according to the dose-survival curve (Table 1).

As shown in Table 1, the in vitro antitumor activities of compounds **1**−**3** against two tumor cell lines were generally better than those of NBDHEX derivative **L1**, Ru-con (without NBDHEX group), and cisplatin, with the order of corresponding cytotoxic activities of **3** > **2** > **1**, suggesting that both GST inhibitor NBDHEX and ruthenium skeleton played critical roles in cytotoxicity. Among them, compound **3** displayed the strongest cytotoxicity toward tumor cells: the in vitro cytotoxicity of compound **3** against A549 and MCF-7 was 13.8 and 2.1 times active, respectively, as compared with cisplatin, increased by 2.2 and 2.1 times, respectively, as compared with NBDHEX derivative **L1**. In addition, the in vitro cytotoxicity of compound **3** against A549 and MCF-7 was 16.2- and 2.6-fold more potent than that of Ru-con, respectively. Moreover, the cytotoxicity of compound **3** against human normal liver cells was significantly lower than that of cisplatin, with the selectivity factors (SF values) of 17.6 and 4.7 relative to A549 and MCF-7, respectively, indicating that compound **3** has advantages in the selectivity between normal and tumor cells. On the contrary, the NBDHEX derivative **L1** seemed to have higher cytotoxic activity on human normal hepatocytes.

In conclusion, complex **3** exhibits excellent cytotoxic activity on the tested cancer cell lines, especially A549 cell line, together with high selectivity between tumor cells and normal cells. Thus, A549 cell line has been chosen as a tumor model to investigate the mode of actions of the resulting ruthenium complexes in the subsequent study.

Live and Dead Cell Staining Study. To further confirm the cytotoxicity of complexes **1**−**3** on tumor cells visually, the live and dead cell staining study was performed by the Calcein-AM/PI double-staining assay. As demonstrated before,[54] Calcein-AM could penetrate the membrane of living cells and be hydrolyzed by intracellular esterases to produce Calcein with strong green fluorescence, while propidium iodide (PI) can only enter the dead cells and intercalate with DNA to form a fluorescent complex. Obviously, A549 cells in the control group exhibited high viability as indicated by the intense green fluorescence (Figure 2), while the cells treated with ligand **L1**, complexes **1**−**3**, and Ru-con showed strong red fluorescence, indicating that the tested compounds could effectively induce the death of A549 cells, especially complex **3** with no green fluorescence observed, which was consistent with the cytotoxicity results of the MTT assay to some extent.

Density Functional Theory Calculations. To explore the potential influence of the arene groups on the cytotoxicity of complexes **1**−**3**, the structures and electronic properties of the compounds were calculated by density functional theory (DFT) methods (Figure 3). The optimized structures displayed that the distances of Ru−Cl bond were increased from complex **1** to **3** with values of 2.413, 2.424, and 2.432 Å, respectively, possibly because of the increased electron density of complex **3** at the Ru(II) center. The increased distance of the Ru−Cl bond of complex **3** may be beneficial for the leaving of the chloride ion and accelerate its chemical reactivity. The EPSs showed that the NBDHEX moieties and Cl atoms are electron-rich sites of compounds **1**−**3**. Distinctly, the electron density around the Ru(II) center in complex **3** is higher than those of complexes **1** and **2** as visualized by the relatively light blue color, further confirming the increased electron density of complex **3** at Ru(II) center.

Kinetics of Hydrolysis. It has been reported that hydrolysis has a substantial influence on the cytotoxicity of the organometallic Ru(II)−arene complexes since it is thought to be the activation step before they covalently bind to the therapeutic targets.[55,56] When chloride in complexes **1**−**3** was substituted by water molecule, the absorbance change of LMCT (ligand-to-metal charge-transfer) band could be observed. Therefore, the hydrolysis behaviors of compounds **1**−**3** were investigated by observing the time-dependent changes in UV/vis absorption bands (Figure 4), and 246 nm was chosen for the kinetic analysis. The absorbance−time trace observed for complexes **1**−**3** fitted well to a monoexponential function, and the hydrolysis rate constants were calculated. According to the data shown in Table 2, the *k* values increased by factors of 3.54 and 2.98 on going from complex **3** to complexes **1** and **2**, respectively, demonstrating that complex **3** has the fastest hydrolysis rate.

https://doi.org/10.1021/acs.inorgchem.1c01482
Inorg. Chem. XXXX, XXX, XXX−XXX

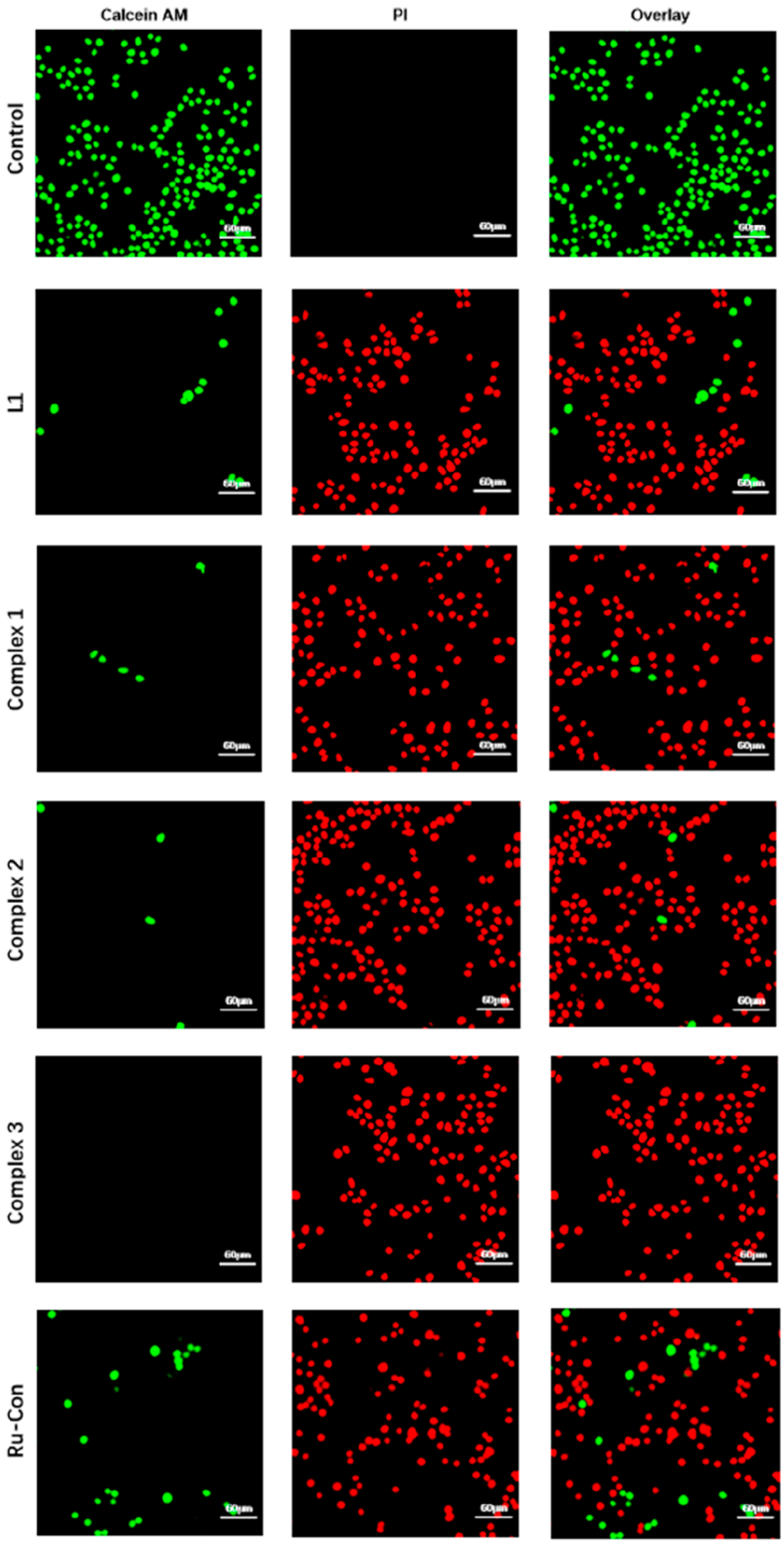

Figure 2. Live/dead cell staining of A549 cells induced by ligand **L1**, complexes **1**−**3**, and Ru-con at the concentration of 30 μM for 24 h.

It has been demonstrated that the electron density at Ru(II) center has a significant impact on the kinetic property of the Ru(II) complex, and increased electron density at Ru(II) facilitates the substitution of halide by water.[57,58] Sadler has proposed that tuning the chemical reactivity of the organometallic ruthenium−arene compounds via electronic effect could be a useful method for the design of an effective anticancer agent.[59] Therefore, complex **3** with the fastest hydrolysis rate among tested compounds could be attributed to the improved electron density at the Ru(II) center from the hexamethylbenzene group. Furthermore, the increased hydrolysis rate of complex **3** may be beneficial for its activation and interaction with the therapeutic target, thus resulting in improved cytotoxicity as compared with complexes **1** and **2**.

https://doi.org/10.1021/acs.inorgchem.1c01482
Inorg. Chem. XXXX, XXX, XXX−XXX

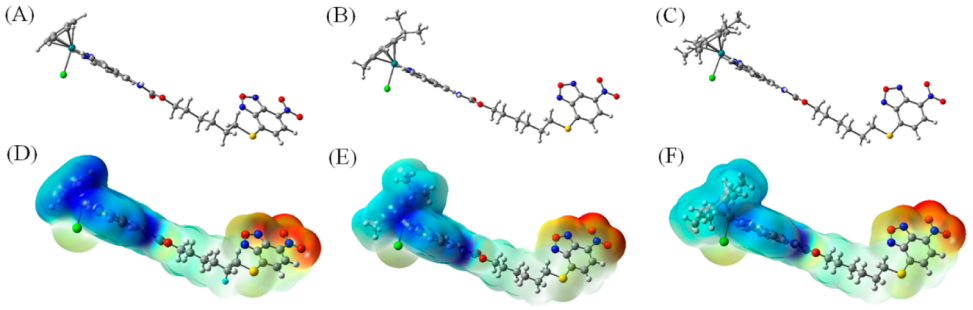

Figure 3. Structures (A−C) and EPSs (D−F) for complexes **1**−**3**. EPS surfaces (from −0.010 au in red to +0.135 au in blue) mapped on electron density (isovalue 0.004 au) of the molecules.

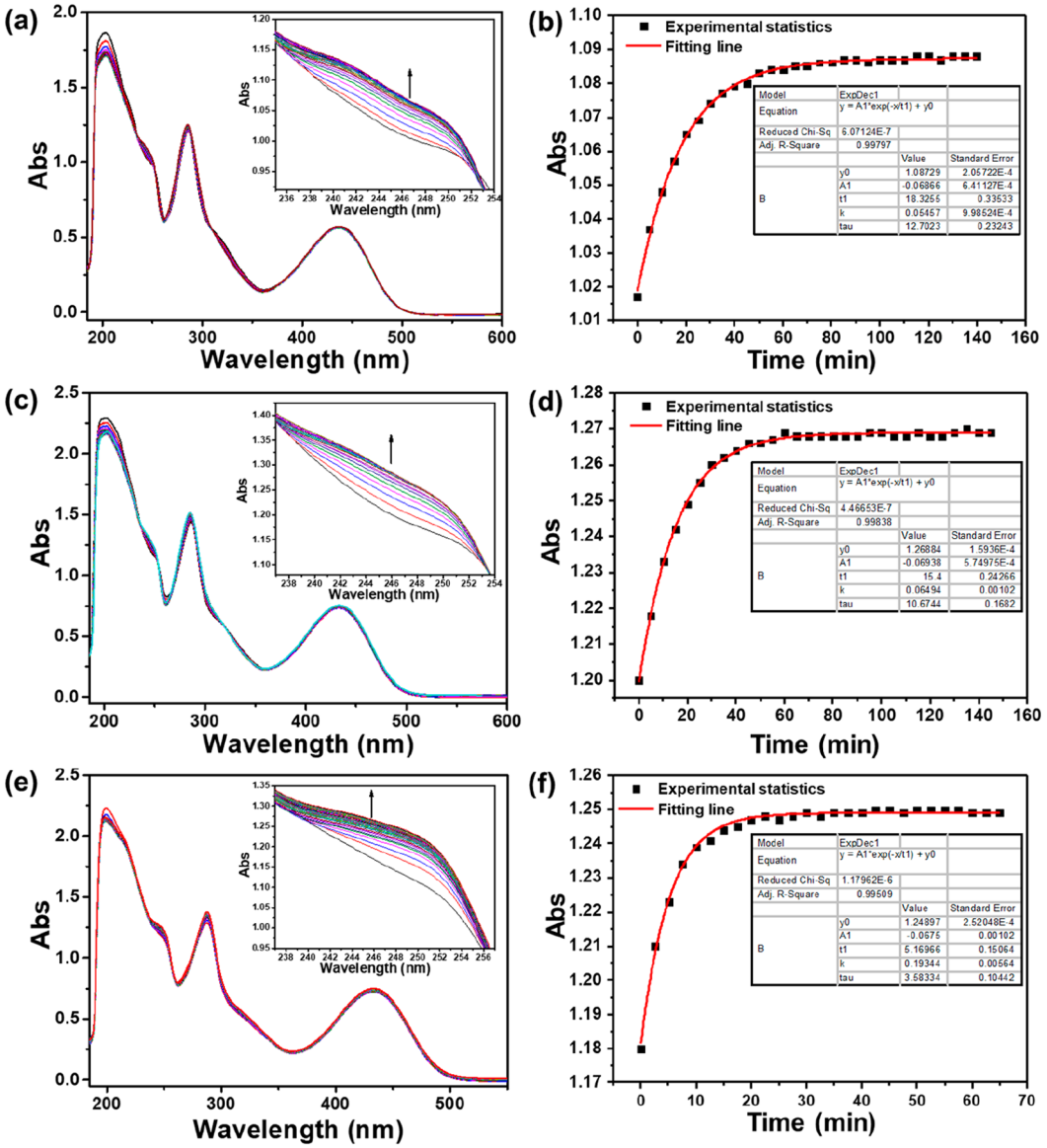

Figure 4. Time-dependent UV−vis spectra for the aquation of 0.05 mM complexes **1** (a), **2** (c), and **3** (a) (95% H_2O/5% MeOH). Absorbance−time trace (246 nm) and monoexponential fit obtained for the hydrolysis of complexes **1** (b), **2** (d), and **3** (f) at 310 K.

Inhibition of GST Activity. As illustrated in Figure 5, the residual activity of GST extracted from A549 cells after treatment with different concentrations of tested compounds was expressed as percentage (%) of control. In Figure 5, it can be noted that ligand **L1** showed similar GST inhibitory activity (14.0−56.2%) as compared to its precursor NBDHEX (16.2−60.5%) at the tested concentrations. Notably, ruthenium complexes **1** (7.6−42.4%) and **2** (6.0−40.1%) with benzene and *p*-cymene moieties, respectively, possessed similar GST inhibitory activity, whereas complex **3** bearing the hexamethyl-

https://doi.org/10.1021/acs.inorgchem.1c01482
Inorg. Chem. XXXX, XXX, XXX−XXX

Table 2. Hydrolysis Rate Constants (k) and Half-Lives ($t_{1/2}$) of Complexes 1−3 (95% H_2O/5% MeOH) at 310 K

complex	1	2	3
k (10^{-4} s^{-1})	9.10	10.82	32.24
$t_{1/2}$ (min)	12.70	10.67	3.58

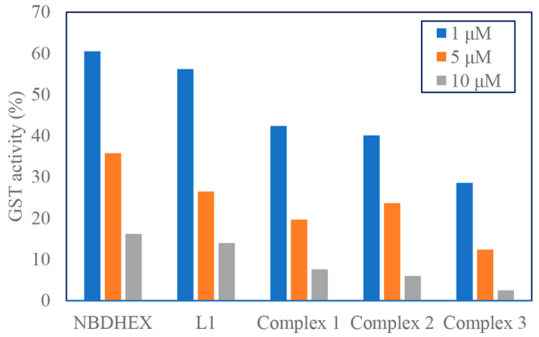

Figure 5. Residual GST activity in A549 cell line after treatment with different concentrations of tested compounds expressed as percentage (%) of control (no inhibitory activity of GST observed in Ru-con).

benzene moiety exhibited the highest GST inhibitory activity (2.5−28.6%) among the tested compounds. The order of the abilities of tested compounds inhibiting GSTs was **3** > **2** ≈ **1** > **L1** ≈ NBDHEX, which was consistent with the results of the in vitro cytotoxicity. It can be inferred that the introduction of NBDHEX on ruthenium(II) complexes can enhance the ability of resulting complexes inhibiting GSTs.

Cellular Accumulation. The cellular accumulation images of complexes in A549 cells were investigated by using laser scanning confocal microscopy (LSCM). As shown in Figure 6, compounds **1**−**3** could effectively enter the A549 cells with the intense green intracellular fluorescence. Remarkably, all the compounds were distributed in the cytoplasm of A549 cells, thus implying that mitochondria may be the therapeutic target of compounds **1**−**3**

To further investigate the correlation between biological activity and cellular accumulation, the intracellular ruthenium accumulation of complexes **1**−**3** (30 μM) in A549 cells was tested by ICP-MS spectra after 6 and 12 h incubation. As shown in Table 3, the relative sequence of cellular uptake of complexes **1**−**3** in A549 cells after 6 h incubation was **3** > **2** > **1** ≫ Ru-Con, which was in accordance with the in vitro cytotoxicity and log P_{OW} results. Moreover, it was found that the cellular uptake of complexes **1**−**3** in A549 cells after 12 h incubation was increased compared with those after 6 h incubation, indicating that the cellular accumulation of complexes **1**−**3** in A549 cells exhibited time dependence behavior.

Table 3. Cellular Accumulation of Complexes 1−3 (30 μM) in A549 Cells after 6 and 12 h Incubation

	Ru (ng/10^6 cells)[a]	
compound	6 h	12 h
1	201 ± 15	275 ± 18
2	240 ± 20	307 ± 21
3	328 ± 24	465 ± 32
Ru-Con	49 ± 3	62 ± 4

[a]Values represent the mean ± SD from three independent experiments by ICP-MS spectra.

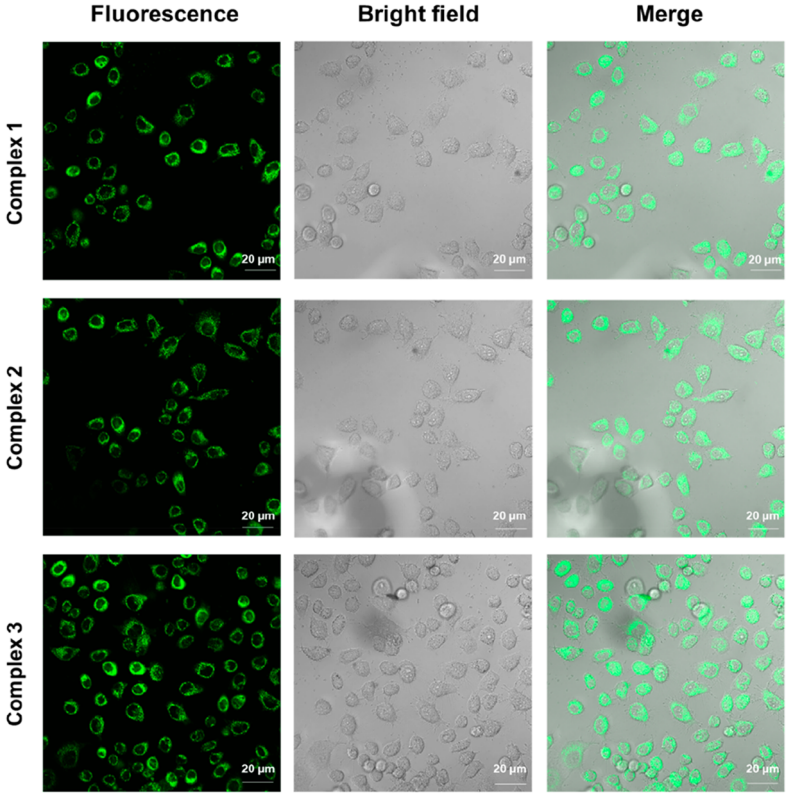

Figure 6. Confocal fluorescence images of A549 cells incubated with complexes **1**−**3** (5 μM) for 4 h.

https://doi.org/10.1021/acs.inorgchem.1c01482
Inorg. Chem. XXXX, XXX, XXX−XXX

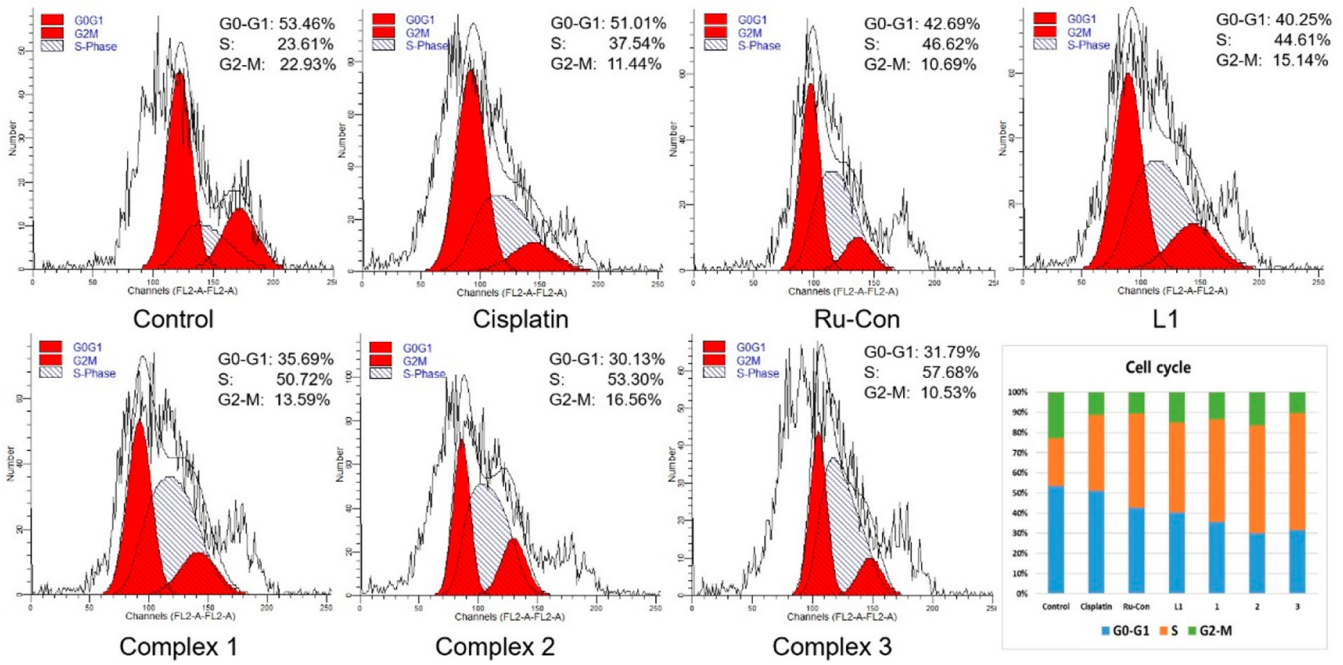

Figure 7. Flow cytometry analysis for cell cycle distributions of A549 cells induced by ligand **L1**, complexes **1**−**3**, cisplatin, and Ru-con at a concentration of 30 μM for 24 h.

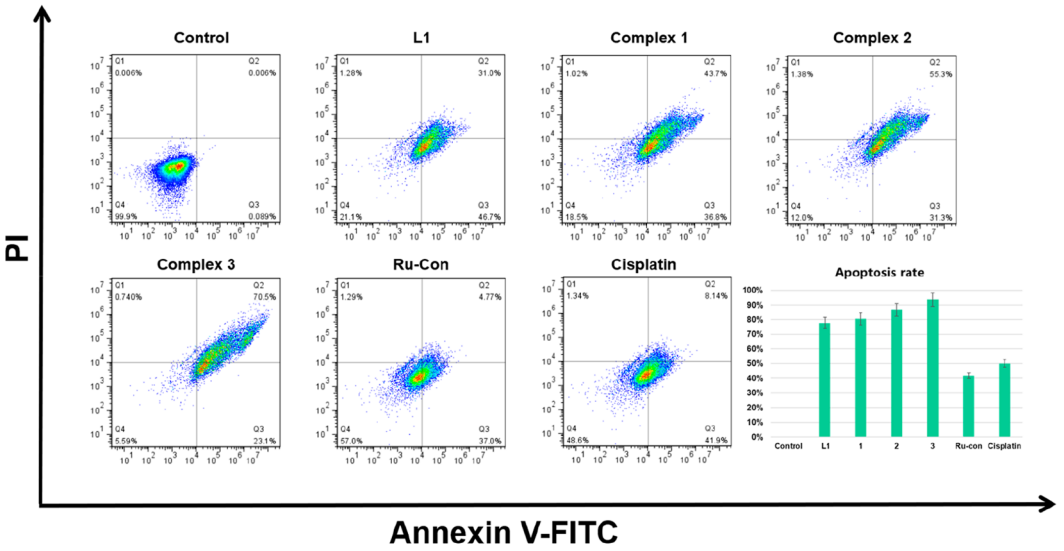

Figure 8. Flow cytometry analysis for apoptosis of A549 cells induced by ligand **L1**, complexes **1**−**3**, cisplatin, and Ru-con at a concentration of 30 μM for 24 h.

Cell Cycle Arrest. The perturbation effects of complexes **1**−**3** on the cell cycle progression of A549 cells together with ligand **L1**, Ru-con, and cisplatin as contrasts were analyzed by flow cytometry. The results of cell cycle are shown in Figure 7. It can be noted that the cell cycle of A549 cells was arrested in the S phase after incubation with ligand **L1** (44.61%), complexes **1**−**3** (50.72−57.68%), Ru-con (46.62%), and cisplatin (37.54%) compared with negative control (23.61%). Anticancer effects of platinum-based drugs have been proved to be mediated by irreversible DNA damage,[3] and furthermore, studies have shown that Ru(II) complexes can bind to DNA and induce apoptosis,[4,60] which was inferred to be the reason for the similar effect caused by Ru-con and cisplatin. In addition, the cell cycle distributions in the S phase were 46.62% and 44.61% after treatment with Ru-con and ligand **L1**, respectively, both of which were higher than that of cisplatin (37.54%). Notably, the cell cycle block effects of complexes **1**−**3** on the S phase (50.72−57.68%) were further strengthened compared with the two precursor compounds **L1** and **Ru-con**, among which the complex **3**-induced S phase arrest showed the highest distribution of 57.68%, whereas the complex 3-induced G2/M phase arrest was only 10.53% distribution.

Apoptosis Study. The necrosis or apoptosis of A549 tumor cells induced by complexes **1**−**3** was detected by using the Annexin V-FITC/PI cell apoptosis detection kit (Roche) and flow cytometry. As shown in Figure 8, complexes **1**−**3** produced high incidences of early to late apoptosis in A549 cells (80.5−93.6%) compared with the untreated cells

https://doi.org/10.1021/acs.inorgchem.1c01482
Inorg. Chem. XXXX, XXX, XXX−XXX

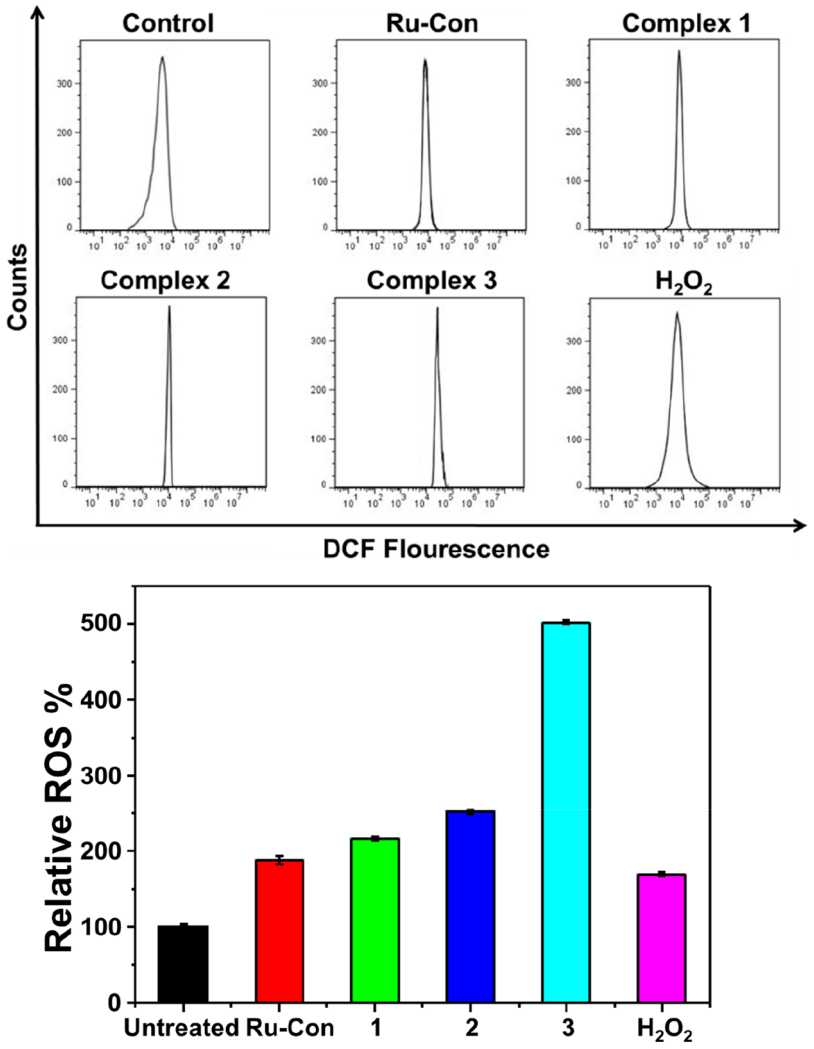

Figure 9. ROS levels of A549 cells induced by ligand **L1**, complexes **1**−**3**, and Ru-con.

(control), demonstrating that complexes **1**−**3** induce cancer cell death via an apoptotic pathway. Significantly, complexes **1**−**3** increased the apoptotic rates of A549 cells as compared with those of ligand **L1** (77.7%), Ru-con (41.8%), and cisplatin (50.0%), especially complex **3**, which induce A549 cell apoptosis with the highest apoptosis population among the tested compounds, further confirming the excellent anticancer activity of complex **3**.

ROS Production. Studies have revealed that ROS (reactive oxygen species) mainly generated in mitochondria as highly reactive molecules play a crucial role in cell proliferation and apoptosis induced by chemotherapeutic drugs. It is also reported that Ru(II) complexes can induce apoptosis and migration inhibition of A549 tumor cells by targeting mitochondria through mitochondrial related events, including mitochondrial membrane permeability and ROS production.[35,61] Therefore, the ROS probe H_2DCFDA (2,7-dichlorodihydrofluorescein diacetate) was used to detect the ROS production level in A549 cells induced by complexes **1**−**3**. DCFH-DA is a nonfluorescent indicator of ROS, but it can be oxidized to DCF with strong fluorescence in A549 cells. The fluorescence intensity was measured by flow cytometry (Ex = 485 nm, Em = 535 nm). As shown in Figure 9, compounds **1**−**3** could effectively induce ROS production in A549 cells, and the relative order of ROS levels induced by tested compounds was **3** > **2** > **1** > Ru-con, among which complex **3** had the highest ROS production level.

Mitochondrial Membrane Potential Study. The loss of mitochondrial membrane potential caused by the intact mitochondrial membrane being disrupted can induce the cascade of the apoptotic pathway by releasing the pro-apoptotic factors from mitochondria.[35,62] The JC-10 fluorescent probe, a water-soluble derivative of JC-1, has been widely used in mitochondrial membrane potential ($\Delta\Psi$m, MMP) studies. In normal cells, JC-10 selectively aggregates in the mitochondrial matrix to form reversible red fluorescent polymers (Ex = 525 nm, Em = 590 nm). Owing to the decrease or loss of $\Delta\Psi$m in unhealthy mitochondria of cells, JC-10 changes from polymer to monomer in the cytoplasm and produces green fluorescence (Ex = 490 nm, Em = 530 nm).

It can be seen in Figure 10 that the green fluorescent monomers in A549 cells treated with Ru-con, ligand **L1**, and complexes **1**−**3** obviously increased compared with the control group, indicating the decrease of mitochondrial membrane potential. Among those, complexes **1**−**3** could cause more mitochondrial depolarization and more decrease of mitochondrial membrane potential than others.

https://doi.org/10.1021/acs.inorgchem.1c01482
Inorg. Chem. XXXX, XXX, XXX−XXX

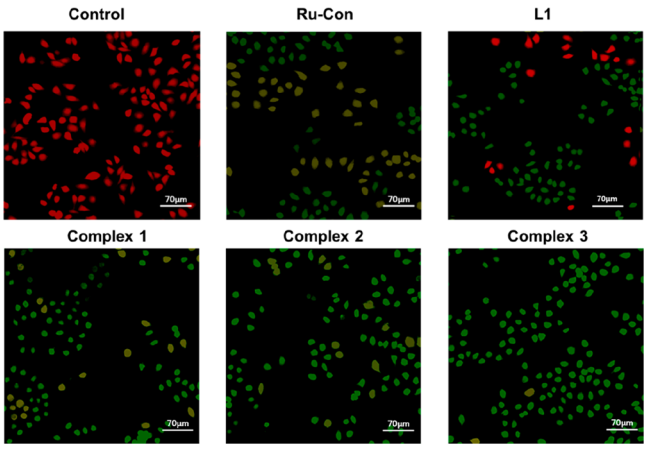

Figure 10. Mitochondrial membrane potential image of A549 cells treated with ligand **L1**, complexes **1**−**3**, and Ru-con.

Western Blot. To further investigate the mechanism of action of the newly synthesized compounds by mitochondrial apoptotic pathway, the effect of compounds on the expression of proteins involved in mitochondrial apoptotic pathway (Bax and Bcl-2) in A549 cells was detected by Western blot analysis. As shown in Figure 11, as compared with control group and

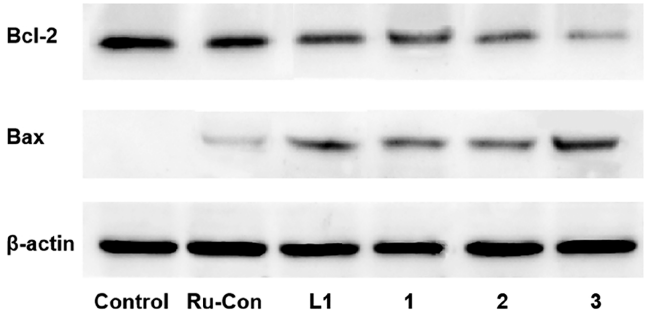

Figure 11. A549 cells treated with ligand **L1**, complexes **1**−**3**, and Ru-con for 24 h were examined for the expression of Bcl-2 and Bax proteins by Western blot analysis.

Ru-con, the expression levels of antiapoptotic Bcl-2 in A549 cells were significantly downregulated after incubation with complexes **1**−**3** functionalized with NBDHEX, while the expression levels of pro-apoptotic Bax were upregulated, suggesting that complexes **1**−**3** probably induced cell apoptosis by mitochondrial apoptotic pathway. In addition, among the tested compounds, complex **3** revealed the highest expression of Bax and lowest expression of Bcl-2, which was in accordance with the results of ROS production and $\Delta\Psi$m study.

CONCLUSIONS

In conclusion, three arene−Ru(II) GST inhibitor conjugates with different arene ligands have been designed and synthesized aiming to improve the pharmacological profiles of the organometallic Ru(II)−arene complex. The newly prepared complexes **1**−**3** exhibited considerable in vitro cytotoxicity against the tested cancer cell lines, superior to either unfunctionalized complex Ru-Con or ligand **L1** alone, suggesting that Ru−arene complex and NBDHEX may have a positive synergistic effect on cancer cells. Moreover, complex **3** with more alkyl groups in the arene ligand displayed the highest in vitro anticancer activity among the tested compounds. DFT calculations and hydrolysis results indicated that complex **3** has the fastest hydrolysis rate as compared with complexes **1** and **2** due to the improved electron density at the Ru(II) center, which may be beneficial for the activation of complex **3**. Most importantly, complexes **1**−**3** showed much less cytotoxicity than cisplatin and ligand **L1** against the normal LO2 cells, suggesting the potential selective cytotoxicity of the prepared complexes toward cancer cell lines. Further studies revealed that complexes **1**−**3** may induce cell death through the mitochondrial apoptotic pathway. Thus, the introduction of GST inhibitor to the chelate ligand in the organometallic Ru(II) complex is an effective way to increase its activity and selectivity against cancer cells, and modification of the arene ligands can further improve the chemical and pharmacological property of the resulting arene−Ru(II) complex.

ASSOCIATED CONTENT

Supporting Information

The Supporting Information is available free of charge at https://pubs.acs.org/doi/10.1021/acs.inorgchem.1c01482.

Synthetic procedures and characterization of ligand **L1** and complexes **1**−**3** and other experimental details (PDF)

AUTHOR INFORMATION

Corresponding Author

Yanyan Sun − *School of Chemistry and Life Sciences, Suzhou University of Science and Technology, Suzhou 215009, China;* orcid.org/0000-0002-4398-4703; Email: sunyy0628@163.com

Authors

Tianyu Han − *School of Chemistry and Chemical Engineering, Southeast University, Nanjing 211189, China*

Yuying Wu − *School of Chemistry and Chemical Engineering, Southeast University, Nanjing 211189, China*

Weinan Han − *School of Chemistry and Life Sciences, Suzhou University of Science and Technology, Suzhou 215009, China*

Kaiwen Yan − *School of Chemistry and Chemical Engineering, Southeast University, Nanjing 211189, China*

Jian Zhao − *School of Chemistry and Chemical Engineering, Southeast University, Nanjing 211189, China;* orcid.org/0000-0002-9365-7727

Complete contact information is available at: https://pubs.acs.org/10.1021/acs.inorgchem.1c01482

Notes

The authors declare no competing financial interest.

ACKNOWLEDGMENTS

We thank the National Natural Science Foundation of China (Grants 21401137 and 21601034) for financial support. The National College Students' innovation and entrepreneurship training program (Grant 201910332008Z) is also appreciated.

REFERENCES

(1) Johnstone, T. C.; Suntharalingam, K.; Lippard, S. J. The Next generation of platinum drugs: targeted Pt (II) agents, nanoparticle delivery, and Pt (IV) prodrugs. *Chem. Rev.* **2016**, *116*, 3436−3486.

https://doi.org/10.1021/acs.inorgchem.1c01482
Inorg. Chem. XXXX, XXX, XXX−XXX

(2) Wheate, N. J.; Walker, S.; Craig, G. E.; Oun, R. The status of platinum anticancer drugs in the clinic and in clinical trials. *Dalton Trans.* **2010**, *39*, 8113−8127.
(3) Kelland, L. The resurgence of platinum-based cancer chemotherapy. *Nat. Rev. Cancer* **2007**, *7*, 573−584.
(4) Yan, Y. K.; Melchart, M.; Habtemariam, A.; Sadler, P. J. Organometallic chemistry, biology and medicine: ruthenium arene anticancer complexes. *Chem. Commun.* **2005**, 4764−4776.
(5) Meier-Menches, S. M.; Gerner, C.; Berger, W.; Hartinger, C. G.; Keppler, B. K. Structure-activity relationships for ruthenium and osmium anticancer agents-towards clinical development. *Chem. Soc. Rev.* **2018**, *47*, 909−928.
(6) Alessio, E.; Mestroni, G.; Bergamo, A.; Sava, G. Rutheniu antimetastatic agents. *Curr. Top. Med. Chem.* **2004**, *4*, 1525−1535.
(7) Zeng, L.; Gupta, P.; Chen, Y.; Wang, E.; Ji, L.; Chao, H.; Chen, Z.-S. The development of anticancer ruthenium (II) complexes: from single molecule compounds to nanomaterials. *Chem. Soc. Rev.* **2017**, *46*, 5771−5804.
(8) Lin, Y.; Wang, J.; Zheng, W.; Luo, Q.; Wu, K.; Du, J.; Zhao, Y.; Wang, F. Organometallic ruthenium anticancer complexes inhibit human peroxiredoxin I activity by binding to and inducing oxidation of its catalytic cysteine residue. *Metallomics* **2019**, *11*, 546−555.
(9) Ribeiro, G. H.; Guedes, A.; de Oliveira, T. D.; de Correia, C.; Colina-Vegas, L.; Lima, M. A.; Nóbrega, J. A.; Cominetti, M. R.; Rocha, F. V.; Ferreira, A. G.; Castellano, E. E.; Teixeira, F. R.; Batista, A. A. Ruthenium(II) Phosphine/Mercapto Complexes: Their in Vitro Cytotoxicity Evaluation and Actions as Inhibitors of Topoisomerase and Proteasome Acting as Possible Triggers of Cell Death Induction. *Inorg. Chem.* **2020**, *59*, 15004−15018.
(10) Roy, N.; Sen, U.; Madaan, Y.; Muthukumar, V.; Varddhan, S.; Sahoo, S. K.; Panda, D.; Bose, B.; Paira, P. Mitochondria-Targeting Click-Derived Pyridinyltriazolylmethylquinoxaline-Based Y-Shaped Binuclear Luminescent Ruthenium(II) and Iridium(III) Complexes as Cancer Theranostic Agents. *Inorg. Chem.* **2020**, *59*, 17689−17711.
(11) Hanif, M.; Nazarov, A. A.; Legin, A.; Groessl, M.; Arion, V. B.; Jakupec, M. A.; Tsybin, Y. O.; Dyson, P. J.; Keppler, B. K.; Hartinger, C. G. Maleimide-functionalised organoruthenium anticancer agents and their binding to thiol-containing biomolecules. *Chem. Commun.* **2012**, *48*, 1475−1477.
(12) Zhao, J.; Li, W.; Gou, S.; Li, S.; Lin, S.; Wei, Q.; Xu, G. Hypoxia-targeting organometallic Ru(II)-arene complexes with enhanced anticancer activity in hypoxic cancer cells. *Inorg. Chem.* **2018**, *57*, 8396−8403.
(13) Poynton, F. E.; Bright, S. A.; Blasco, S.; Williams, D. C.; Kelly, J. M.; Gunnlaugsson, T. The development of ruthenium (II) polypyridyl complexes and conjugates for in vitro cellular and in vivo applications. *Chem. Soc. Rev.* **2017**, *46*, 7706−7756.
(14) Li, J.; Tian, M.; Tian, Z.; Zhang, S.; Yan, C.; Shao, C.; Liu, Z. Half-sandwich iridium (III) and ruthenium (II) complexes containing P∧P-chelating ligands: A new class of potent anticancer agents with unusual redox features. *Inorg. Chem.* **2018**, *57*, 1705−1716.
(15) Du, J.; Kang, Y.; Zhao, Y.; Zheng, W.; Zhang, Y.; Lin, Y.; Wang, Z.; Wang, Y.; Luo, Q.; Wu, K.; Wang, F. Synthesis, Characterization, and in Vitro Antitumor Activity of Ruthenium(II) Polypyridyl Complexes Tethering EGFR-Inhibiting 4-Anilinoquinazolines. *Inorg. Chem.* **2016**, *55*, 4595−4605.
(16) Vock, C. A.; Ang, W. H.; Scolaro, C.; Phillips, A. D.; Lagopoulos, L.; Juillerat-Jeanneret, L.; Sava, G.; Scopelliti, R.; Dyson, P. J. Development of Ruthenium Antitumor Drugs that Overcome Multidrug Resistance Mechanisms. *J. Med. Chem.* **2007**, *50*, 2166−2175.
(17) Zhao, J.; Zhang, D.; Hua, W.; Li, W.; Xu, G.; Gou, S. Anticancer Activity of Bifunctional Organometallic Ru (II) Arene Complexes Containing a 7-Hydroxycoumarin Group. *Organometallics* **2018**, *37*, 441−447.
(18) Zhao, J.; Li, S.; Wang, X.; Xu, G.; Gou, S. Dinuclear organoruthenium complexes exhibiting antiproliferative activity through DNA damage and a reactive-oxygen-species-mediated endoplasmic reticulum stress pathway. *Inorg. Chem.* **2019**, *58*, 2208−2217.
(19) Xue, X.; Qian, C.; Tao, Q.; Dai, Y.; Lv, M.; Dong, J.; Su, Z.; Qian, Y.; Zhao, J.; Liu, H.; Guo, Z. Using bioorthogonally catalyzed lethality strategy to generate mitochondria-targeting antitumor metallodrugs in vitro and in vivo. *Natl. Sci. Rev.* **2020**, nwaa286.
(20) Bergamo, A.; Sava, G. Ruthenium anticancer compounds: myths and realities of the emerging metal-based drugs. *Dalton Trans.* **2011**, *40*, 7817−7823.
(21) Hartinger, C. G.; Jakupec, M. A.; Zorbas-Seifried, S.; Groessl, M.; Egger, A.; Berger, W.; Zorbas, H.; Dyson, P. J.; Keppler, B. K. KP1019, a new redox-active anticancer agent-preclinical development and results of a clinical phase I study in tumor patients. *Chem. Biodiversity* **2008**, *5*, 2140−2155.
(22) Riedl, C. A.; Flocke, L. S.; Hejl, M.; Roller, A.; Klose, M. H.; Jakupec, M. A.; Kandioller, W.; Keppler, B. K. Introducing the 4-Phenyl-1, 2, 3-Triazole Moiety as a Versatile Scaffold for the Development of Cytotoxic Ruthenium (II) and Osmium (II) Arene Cyclometalates. *Inorg. Chem.* **2017**, *56*, 528−541.
(23) Trondl, R.; Heffeter, P.; Kowol, C. R.; Jakupec, M. A.; Berger, W.; Keppler, B. K. NKP-1339, the first ruthenium-based anticancer drug on the edge to clinical application. *Chem. Sci.* **2014**, *5*, 2925−2932.
(24) Alessio, E. 30 years of the drug candidate NAMI-A and the myths in the field of ruthenium anticancer compounds: A personal perspective. *Eur. J. Inorg. Chem.* **2017**, *2017*, 1549−1560.
(25) Alessio, E.; Messori, L. NAMI-A and KP1019/1339, two iconic ruthenium anticancer drug candidates face-to-face: a case story in medicinal inorganic chemistry. *Molecules* **2019**, *24*, 1995.
(26) Guichard, S.; Else, R.; Reid, E.; Zeitlin, B.; Aird, R.; Muir, M.; Dodds, M.; Fiebig, H.; Sadler, P.; Jodrell, D. Anti-tumour activity in non-small cell lung cancer models and toxicity profiles for novel ruthenium (II) based organo-metallic compounds. *Biochem. Pharmacol.* **2006**, *71*, 408−415.
(27) Scolaro, C.; Bergamo, A.; Brescacin, L.; Delfino, R.; Cocchietto, M.; Laurenczy, G.; Geldbach, T. J.; Sava, G.; Dyson, P. J. In vitro and in vivo evaluation of ruthenium(II)-arene PTA complexes. *J. Med. Chem.* **2005**, *48*, 4161−4171.
(28) Murray, B. S.; Babak, M. V.; Hartinger, C. G.; Dyson, P. J. The development of RAPTA compounds for the treatment of tumors. *Coord. Chem. Rev.* **2016**, *306*, 86−114.
(29) Rausch, M.; Dyson, P. J.; Nowak-Sliwinska, P. Recent Considerations in the Application of RAPTA-C for Cancer Treatment and Perspectives for Its Combination with Immunotherapies. *Adv. Ther.* **2019**, *2*, 1900042.
(30) Sersen, S.; Kljun, J.; Kryeziu, K.; Panchuk, R.; Alte, B.; Korner, W.; Heffeter, P.; Berger, W.; Turel, I. Structure-related mode-of-action differences of anticancer organoruthenium complexes with β-diketonates. *J. Med. Chem.* **2015**, *58*, 3984−3996.
(31) Chow, M. J.; Licona, C.; Pastorin, G.; Mellitzer, G.; Ang, W. H.; Gaiddon, C. Structural tuning of organoruthenium compounds allows oxidative switch to control ER stress pathways and bypass multidrug resistance. *Chem. Sci.* **2016**, *7*, 4117−4124.
(32) Chow, M. J.; Alfiean, M.; Pastorin, G.; Gaiddon, C.; Ang, W. H. Apoptosis-independent organoruthenium anticancer complexes that overcome multidrug resistance: self-assembly and phenotypic screening strategies. *Chem. Sci.* **2017**, *8*, 3641−3649.
(33) Anthony, E. J.; Bolitho, E. M.; Bridgewater, H. E.; Carter, O. W. L.; Donnelly, J. M.; Imberti, C.; Lant, E. C.; Lermyte, F.; Needham, R. J.; Palau, M.; Sadler, P. J.; Shi, H. Y.; Wang, F. X.; Zhang, W. Y.; Zhang, Z. J. Metallodrugs are unique: opportunities and challenges of discovery and development. *Chem. Sci.* **2020**, *11*, 12888−12917.
(34) Batchelor, L. K.; Paunescu, E.; Soudani, M.; Scopelliti, R.; Dyson, P. J. Influence of the linker length on the cytotoxicity of homobinuclear ruthenium (II) and gold (I) complexes. *Inorg. Chem.* **2017**, *56*, 9617−9633.
(35) Xu, Z. S.; Kong, D. L.; He, X. D.; Guo, L. H.; Ge, X. X.; Liu, X. C.; Zhang, H. R.; Li, J. J.; Yang, Y. L.; Liu, Z. Mitochondria-targeted half-sandwich ruthenium(II) diimine complexes: anticancer and

https://doi.org/10.1021/acs.inorgchem.1c01482
Inorg. Chem. XXXX, XXX, XXX−XXX

antimetastasis via ROS-mediated signaling. *Inorg. Chem. Front.* **2018**, *5*, 2100−2105.
(36) Liu, Q.; Liu, Z.; Hua, W.; Gou, S. Discovery of 6-(7-Nitro-2,1,3-benzoxadiazol-4-ylthio)hexanol Derivatives as Glutathione Transferase Inhibitors with Favorable Selectivity and Tolerated Toxicity. *J. Med. Chem.* **2021**, *64*, 1701−1712.
(37) Johansson, K.; Ito, M.; Schophuizen, C. M. S.; Thengumtharayil, S. M.; Heuser, V. D.; Zhang, J.; Shimoji, M.; Vahter, M.; Ang, W. H.; Dyson, P. J.; Shibata, A.; Shuto, S.; Ito, Y.; Abe, H.; Morgenstern, R. Characterization of new potential anticancer drugs designed to overcome glutathione transferase mediated resistance. *Mol. Pharmaceutics* **2011**, *8*, 1698−1708.
(38) Singh, R. R.; Reindl, K. M. Glutathione S-Transferases in cancer. *Antioxidants* **2021**, *10*, 701.
(39) Cummins, I.; Wortley, D. J.; Sabbadin, F.; He, Z.; Coxon, C. R.; Straker, H. E.; Sellars, J. D.; Knight, K.; Edwards, L.; Hughes, D.; Kaundun, S. S.; Hutchings, S. J.; Steel, P. G.; Edwards, R. Key role for a glutathione transferase in multiple-herbicide resistance in grass weeds. *Proc. Natl. Acad. Sci. U. S. A.* **2013**, *110*, 5812−5817.
(40) Harshbarger, W.; Gondi, S.; Ficarro, S. B.; Hunter, J.; Udayakumar, D.; Gurbani, D.; Singer, W. D.; Liu, Y.; Li, L.; Marto, J. A.; Westover, K. D. Structural and biochemical analyses reveal the mechanism of glutathione S-transferase Pi 1 inhibition by the anti-cancer compound piperlongumine. *J. Biol. Chem.* **2017**, *292*, 112−120.
(41) Duvoix, A.; Morceau, F.; Delhalle, S.; Schmitz, M.; Schnekenburger, M.; Galteau, M. M.; Dicato, M.; Diederich, M. Induction of apoptosis by curcumin: mediation by glutathione S-transferase P1−1 inhibition. *Biochem. Pharmacol.* **2003**, *66*, 1475−1483.
(42) Lee, K. G. Z.; Babak, M. V.; Weiss, A.; Dyson, P. J.; Nowak-Sliwinska, P.; Montagner, D.; Ang, W. H. Development of an efficient dual-action GST-inhibiting anticancer platinum(IV) prodrug. *ChemMedChem.* **2018**, *13*, 1210−1217.
(43) Agonigi, G.; Riedel, T.; Zacchini, S.; Păunescu, E.; Pampaloni, G.; Bartalucci, N.; Dyson, P. J.; Marchetti, F. Synthesis and Antiproliferative Activity of New Ruthenium Complexes with Ethacrynic-Acid-Modified Pyridine and Triphenylphosphine Ligands. *Inorg. Chem.* **2015**, *54*, 6504−6512.
(44) Chen, H.; Chen, F.; Wang, X.; Gou, S. Multifunctional Pt(IV) complexes containing a glutathione S-transferase inhibitor lead to enhancing anticancer activity and preventing metastasis of osteosarcoma cells. *Metallomics* **2019**, *11*, 317−326.
(45) Paunescu, E.; Soudani, M.; Martin, P.; Scopelliti, R.; Lo Bello, M.; Dyson, P. J. Organometallic Glutathione S-Transferase Inhibitors. *Organometallics* **2017**, *36*, 3313−3321.
(46) Sau, A.; Tregno, F. P.; Valentino, F.; Federici, G.; Caccuri, A. M. Glutathione transferases and development of new principles to overcome drug resistance. *Arch. Biochem. Biophys.* **2010**, *500*, 116−122.
(47) Sezen, B.; Sames, D. Selective and catalytic arylation of N-phenylpyrrolidine: (sp3) C-H bond functionalization in the absence of a directing group. *J. Am. Chem. Soc.* **2005**, *127*, 5284−5285.
(48) Agonigi, G.; Riedel, T.; Gay, M. P.; Biancalana, L.; Oñate, E.; Dyson, P. J.; Pampaloni, G.; Păunescu, E.; Esteruelas, M. A.; Marchetti, F. Arene osmium complexes with ethacrynic acid-modified ligands: synthesis, characterization, and evaluation of intracellular glutathione S-transferase inhibition and antiproliferative activity. *Organometallics* **2016**, *35*, 1046−1056.
(49) Ricci, G.; De Maria, F.; Antonini, G.; Turella, P.; Bullo, A.; Stella, L.; Filomeni, G.; Federici, G.; Caccuri, A. M. 7-Nitro-2,1,3-benzoxadiazole derivatives, a new class of suicide inhibitors for glutathione S-transferases. Mechanism of action of potential anticancer drugs. *J. Biol. Chem.* **2005**, *280*, 26397−26405.
(50) Federici, L.; Lo Sterzo, C.; Pezzola, S.; Di Matteo, A.; Scaloni, F.; Federici, G.; Caccuri, A. M. Structural basis for the binding of the anticancer compound 6-(7-nitro-2,1,3-benzoxadiazol-4-ylthio)hexanol to human glutathione s-transferases. *Cancer Res.* **2009**, *69*, 8025−8034.
(51) De Luca, A.; Pellizzari Tregno, F.; Sau, A.; Pastore, A.; Palumbo, C.; Alama, A.; Cicconi, R.; Federici, G.; Caccuri, A. M. Glutathione S-transferase P1−1 as a target for mesothelioma treatment. *Cancer Sci.* **2013**, *104*, 223−230.
(52) De Luca, A.; Rotili, D.; Carpanese, D.; Lenoci, A.; Calderan, L.; Scimeca, M.; Mai, A.; Bonanno, E.; Rosato, A.; Geroni, C.; Quintieri, L.; Caccuri, A. M. A novel orally active water-soluble inhibitor of human glutathione transferase exerts a potent and selective antitumor activity against human melanoma xenografts. *Oncotarget* **2015**, *6*, 4126−4143.
(53) De Luca, A.; Carpanese, D.; Rapanotti, M. C.; Viguria, T. M.; Forgione, M. A.; Rotili, D.; Fulci, C.; Iorio, E.; Quintieri, L.; Chimenti, S.; Bianchi, L.; Rosato, A.; Caccuri, A. M. The nitrobenzoxadiazole derivative MC3181 blocks melanoma invasion and metastasis. *Oncotarget* **2017**, *8*, 15520−15538.
(54) Li, S.; Zhao, J.; Wang, X.; Xu, G.; Gou, S.; Zhao, Q. Design of a tris-heteroleptic Ru(II) complex with red-Light excitation and remarkably improved photobiological activity. *Inorg. Chem.* **2020**, *59*, 11193−11204.
(55) Zheng, W.; Luo, Q.; Lin, Y.; Zhao, Y.; Wang, X.; Du, Z.; Hao, X.; Yu, Y.; Lv, S.; Ji, L.; et al. Complexation with organometallic ruthenium pharmacophores enhances the ability of 4-anilinoquinazolines inducing apoptosis. *Chem. Commun.* **2013**, *49*, 10224−10226.
(56) Du, J.; Zhang, E.; Zhao, Y.; Zheng, W.; Zhang, Y.; Lin, Y.; Wang, Z.; Luo, Q.; Wu, K.; Wang, F. Discovery of a dual-targeting organometallic ruthenium complex with high activity inducing early stage apoptosis of cancer cells. *Metallomics* **2015**, *7*, 1573−1583.
(57) Dougan, S. J.; Melchart, M.; Habtemariam, A.; Parsons, S.; Sadler, P. J. Phenylazo-pyridine and phenylazo-pyrazole chlorido ruthenium(II) arene complexes: arene loss, aquation, and cancer cell cytotoxicity. *Inorg. Chem.* **2006**, *45*, 10882−10894.
(58) Bugarcic, T.; Habtemariam, A.; Deeth, R. J.; Fabbiani, F. P.; Parsons, S.; Sadler, P. J. Ruthenium(II) arene anticancer complexes with redox-active diamine ligands. *Inorg. Chem.* **2009**, *48*, 9444−9453.
(59) Wang, F.; Habtemariam, A.; van der Geer, E. P.; Fernández, R.; Melchart, M.; Deeth, R. J.; Aird, R.; Guichard, S.; Fabbiani, F. P.; Lozano-Casal, P.; Oswald, I. D.; Jodrell, D. I.; Parsons, S.; Sadler, P. J. Controlling ligand substitution reactions of organometallic complexes: tuning cancer cell cytotoxicity. *Proc. Natl. Acad. Sci. U. S. A.* **2005**, *102*, 18269−18274.
(60) Novakova, O.; Chen, H.; Vrana, O.; Rodger, A.; Sadler, P. J.; Brabec, V. DNA interactions of monofunctional organometallic ruthenium(II) antitumor complexes in cell-free media. *Biochemistry* **2003**, *42*, 11544−11554.
(61) Ye, Y.; Zhang, T.; Yuan, H.; Li, D.; Lou, H.; Fan, P. Mitochondria-Targeted Lupane Triterpenoid Derivatives and Their Selective Apoptosis-Inducing Anticancer Mechanisms. *J. Med. Chem.* **2017**, *60*, 6353−6363.
(62) He, H.; Wang, J.; Wang, H.; Zhou, N.; Yang, D.; Green, D. R.; Xu, B. Enzymatic Cleavage of Branched Peptides for Targeting Mitochondria. *J. Am. Chem. Soc.* **2018**, *140*, 1215−1218.

https://doi.org/10.1021/acs.inorgchem.1c01482
Inorg. Chem. XXXX, XXX, XXX−XXX